Naval Research Laboratory
Washington, DC 20375-5320

NRL/FR/7140--98-9885

Bottom Backscattering Measured Off the Carolina Coast During the Littoral Warfare Advanced Development System Concept Validation Experiment 97 (LWAD SCV 97)

RAYMOND J. SOUKUP

Acoustic Systems Branch
Acoustics Division

June 15, 1998

REPORT DOCUMENTATION PAGE

Form Approved
OMB No. 0704-0188

1. AGENCY USE ONLY *(Leave Blank)*	2. REPORT DATE	3. REPORT TYPE AND DATES COVERED
	June 15, 1998	Interim Report October 1997 to February 1998

4. TITLE AND SUBTITLE

Bottom Backscattering Measured Off the Carolina Coast During the Littoral Warfare Advanced Development System Concept Validation Experiment 97 (LWAD SCV 97)

5. FUNDING NUMBERS

PE - 0603747N

6. AUTHOR(S)

Raymond J. Soukup

7. PERFORMING ORGANIZATION NAME(S) AND ADDRESS(ES)

Naval Research Laboratory
Washington, DC 20375-5320

8. PERFORMING ORGANIZATION REPORT NUMBER

NRL/FR/7140--98-9885

9. SPONSORING/MONITORING AGENCY NAME(S) AND ADDRESS(ES)

Office of Naval Research
Arlington, VA 22217-5660

10. SPONSORING/MONITORING AGENCY REPORT NUMBER

11. SUPPLEMENTARY NOTES

12a. DISTRIBUTION/AVAILABILITY STATEMENT

Approved for public release; distribution is unlimited.

12b. DISTRIBUTION CODE

13. ABSTRACT *(Maximum 200 words)*

Measurements of ocean bottom backscattering were performed in a shallow water environment off the Carolina coast as part of the Littoral Warfare Advanced Development System Concept Validation Experiment 97 (LWAD SCV 97). Scattering strengths were obtained from 1.5 to 4 kHz as a function of grazing angle. The site dependence arising from the presence or absence of a sandy sediment layer was investigated. Scattering strengths in the deeper areas, where sediment had been scoured by Gulf Stream activity and acoustic interactions with the underlying limestone occurred, were in the range of −15 to −20 dB with a slight frequency dependence. Scattering strengths in the presence of an acoustically significant (at least 20 m) sediment layer were in the −25 to −30 dB range and showed no clear frequency dependence. The grazing angle dependence could be fit adequately by assuming a dependence of scattering strength on the sine of the grazing angle.

14. SUBJECT TERMS

Bottom scattering
Sediment wedge
Reverberation
Active sonar
Underwater acoustics

15. NUMBER OF PAGES

26

16. PRICE CODE

17. SECURITY CLASSIFICATION OF REPORT	18. SECURITY CLASSIFICATION OF THIS PAGE	19. SECURITY CLASSIFICATION OF ABSTRACT	20. LIMITATION OF ABSTRACT
UNCLASSIFIED	UNCLASSIFIED	UNCLASSIFIED	UL

NSN 7540-01-280-5500

Standard Form 298 (Rev. 2-89)
Prescribed by ANSI Std 239-18
298-102

CONTENTS

BOTTOM BACKSCATTERING MEASURED OFF THE CAROLINA COAST DURING THE LITTORAL WARFARE ADVANCED DEVELOPMENT SYSTEM CONCEPT VALIDATION EXPERIMENT 97 (LWAD SCV 97)

INTRODUCTION

The Littoral Warfare Advanced Development System Concept Validation 97 (LWAD SCV 97) experiment was conducted off the Carolina coast in September 1997. As a potential source of clutter for active sonar systems in this littoral area, the ocean bottom was characterized to assist in understanding system performance. Direct path (i.e., source to bottom to receiver) measurements of the bottom backscattering strength (BSS) in the 1.5 to 4.0 kHz band were obtained. Figure 1 shows the LWAD SCV 97 test location. Primary test operations, involving the testing of several mid-frequency sonar systems, took place at water depths shallower than 300 m. The bottom scattering experiments were designed to provide inputs to performance models of these systems.

The bottom interaction problem can involve multiple physical processes, all of which may contribute to the measured scattering strength: scattering from the water/sediment interface, scattering in the sediment volume itself, or scattering from the basement or a subsurface layer with a significant impedance mismatch. The frequency and grazing-angle dependence can reflect an enhancement of one mechanism over another, and given the variability of the littoral environment in sediment thickness, composition, and frequency-dependent attenuation, correct physical interpretation of bottom scattering strengths usually requires significant knowledge of the geoacoustic properties and structure of the subbottom. For most of the LWAD SCV 97 test location, the Gulf Stream has scoured the sandy sediment so that minimal cover remains and scattering takes place off the exposed limestone. This leads to some consistency in data taken from different sites. For shallower regions within the test location, where sand cover tends to be significant and results depend on specific characteristics such as sand layer thickness and homogeneity, there is greater potential for variability in frequency and site dependence.

Bottom scattering strength can be calculated by solving the sonar equation in the following form:

$$BSS = RL - SL + TL_s + TL_r - 10\log A \tag{1}$$

where BSS is the scattering strength in dB, RL is the measured reverberation level in dB *re* $(1\mu\text{Pa})^2/\text{Hz}$, SL is the source level in dB *re* $(1\mu\text{Pa})^2/\text{Hz}$ at 1 m, TL_s is the transmission loss from the source to the ensonified patch on the bottom in dB, TL_r is the transmission loss from the ensonified patch on the bottom to the receiver in dB, and A is the area of the ensonified patch in square meters. The BSS results from LWAD SCV 97 were calculated assuming a flat bottom.

Manuscript approved April 17, 1998.

For performance modeling purposes, one would have to calculate the grazing angles of bottom interactions with respect to the actual bathymetry.

During the LWAD SCV 97 test BSS results were obtained at five sites. Data were obtained at seven frequencies (1.5, 2, 2.5, 3, 3.5, 4, and 4.5 kHz) at water depths ranging from 120 to 232 m, typically covering grazing angles of 7 to 30 degrees. The specific site locations for bottom scattering for two different areas within the test location of Fig. 1 are shown in Figs. 2 and 3. These areas are designated as the "north" area and the "south" area throughout this report. Figure 3 also shows the locations (named site B and site Q) where data were collected during an earlier experiment, Littoral Warfare Advanced Development Focused Technology Experiment 96-2 (LWAD FTE 96-2). The sites in the north area were of two types: one with significant sandy sediment thickness (NS), and another where sediment was negligible (NR). In the south area (sites SR1, SR2, and SR3), the primary bottom type was limestone for the starting positions of the runs at the three sites, however, there is evidence that the sandy covering began to influence the site SR1 data as the ship drifted shallower. (Figure 3 shows the ship drift.) Additionally, data from site B with known significant sandy sediment thickness (25 m) were obtained during the LWAD FTE 96-2 test. Figures 2 and 3 also show reference points (ZL and ZLS) where assets were placed for the execution of other events during the LWAD SCV 97 experiment.

BSS measurements were obtained during LWAD FTE 96-2 using a monostatic system with an omnidirectional source (USRD F80) and nine-element vertical line array (VLA) aperture. Results from this test in the 2.0 to 3.5 kHz band were reported by Soukup and Ogden [1]. The LWAD FTE 96-2 test area provided an opportunity to observe the strong dependence in scattering strength level on the presence or absence of a significant sand layer. LWAD FTE 96-2 data could be fit well by assuming a scattering strength proportional to the sine of the grazing angle, with proportionality constants of -24 dB to -32 dB for site B. For sites (including site Q) with sand cover that could not be resolved by a seismic system (i.e., less than 1 m layer thickness), constants of -13 to -16 dB were obtained. These values were compared with bottom backscattering results in the survey article of McCammon [2], generally agreeing with the historical data shown there.

For the LWAD SCV 97 test, efforts were made to

- sample new rock and sandy sites in the north area,
- extend the measurement frequency band to 1.5 to 4.5 kHz,
- use a directional source to reduce high-angle returns, and
- increase the receiving aperture from 9 phones to 16 phones.

System modifications and deployments were designed to obtain a set of grazing angles lower than those obtained from the LWAD FTE 96-2 measurements. Efforts were also made to obtain seismic data (using a chirp sonar system owned by North Carolina State University) in the same locations as the scattering sites to establish the true local thickness of sand cover. Additionally, light bulbs with implosions at specified water depths were dropped during three of the scattering runs to provide additional bottom characterization (i.e., estimates of compressional speed and layer thickness).

This report addresses the site dependence and frequency dependence of the BSS. The results are summarized in the form of an empirical model for grazing angle dependence and compared with the LWAD FTE 96-2 results and the scattering levels described by McCammon [2]. Physics-based

models for rocky bottoms (including the effects of subinterface volume scattering and shear) are currently under development. In the near future, we hope that the rock data, which form a majority of the data presented here, can be well characterized by a physics-based model. Until these models are developed and tested with the type of data collected for this report, the frequency dependence and bottom roughness dependence of rock scattering cannot be well understood. For the areas with sand layers thick enough to prevent ensonification of the bottom, a bottom backscattering model based on geoacoustic information can be used. An example of this is given in Soukup and Edsall [3], where the bottom scattering model of Mourad and Jackson [4] is used.

EXPERIMENT GEOMETRY AND DATA ANALYSIS

The bottom scattering tests were conducted from the research vessel GOSPORT during SCV 97. Figure 4 is a schematic diagram of the geometry. A vertical line array and a source were deployed on a single cable, with the source located 2 m (for the north area measurements) or 4 m (for the south area measurements) above the center of the VLA receiving aperture. This resulted in a nearly monostatic measurement geometry.

The source was a ring-shaped transducer (USRD G81) that gave maximum (over the range of launch angles) root-mean-square source levels ranging from 186 dB (1500 Hz) to 195 dB (3500 Hz). The source beam pattern features a null in the upward direction and some flattening in the downward direction. This beam pattern gave maximum source level for all of the launch directions used to calculate scattering strength, so the deviations from the omnidirectional pattern did not affect the BSS calculation. However, the source directionality does help to mitigate sidelobe interference for very high grazing-angle returns, such as the initial acoustic interactions with the ocean surface and bottom. This allows extension of data validity to lower grazing angles. During most runs, the source was placed successively at two different depths (a subset of 50, 60, and 90 m) and a set of pings was transmitted at each depth to produce two different bands of measured grazing angles. The waveforms were 50 ms gated continuous wave (GCW) signals at frequencies of 1.5, 2.0, 2.5, 3.0, 3.5, 4, and 4.5 kHz. Sets of 8 to 21 identical pings were transmitted at each frequency, with individual pings separated by 15 s. In some cases, a wavetrain was transmitted consisting of four adjacent 50 ms GCW signals in the sequence 2.5, 3.5, 2.0, and 3.0 kHz – the resulting scattering strengths were comparable to those obtained by transmitting the frequencies individually.

The bottom reverberation from the 50 ms pulses was received on either a nine or 16-hydrophone VLA aperture. (The VLA with the 16-hydrophone aperture failed during the performance of the last northern area run; another VLA with a nine-phone aperture was substituted for the southern area.) The hydrophones were spaced at either 21 cm (for the nine-phone aperture) or 15 cm (for the 16-phone aperture), which corresponds to half-wavelength spacings of 3570 Hz and 4920 Hz respectively. Ten and 17 beams with cosine-spaced main response axes were formed from the none and 16-apertures, respectively, with most of the returns of interest coming from downward-looking beams closest to broadside. For LWAD SCV 97, the minimum and maximum horizontal ranges used for a scatterer-to-receiver path were approximately 150 m to 1350 m, respectively. The ensonified area for scattering calculations ranged from 44,000 m^2 (0.04 km^2) to 320,000 m^2 (0.32 km^2).

After beamforming, power spectra were obtained by performing 50 ms Fourier transforms with 50 percent overlap over the length of the reverberation time series. A frequency band representing

the total energy about the zero-Doppler peak was selected, and a time series including only the energy in this band was created for each ping. The direct arrivals for the pings were then temporally aligned and the various pings were averaged to produce a single reverberation curve for each beam and frequency bin. Integration over the roughly zero-Doppler spectral peak produced the total returned power as a function of time and beam. By calculating geometric spreading loss along each ray path, the transmission loss terms to and from the scattering patch were obtained. Finally, the computed beam pattern and raytrace were used to calculate the scattering patch area. From these inputs, BSS was calculated using Eq. (1) as a function of beam, frequency, and grazing angle. Additional details about the processing scheme are given by Ogden and Erskine [5]. The standard deviations due to ping-to-ping variability within the sets of identical transmissions were $\pm$ 2 to 3 dB. The system calibration was worked out to 1 dB accuracy.

BOTTOM SCATTERING RESULTS

Site Dependence

In the LWAD SCV 97 test area, the ocean bottom east of the shelf break features a sedimentary wedge of calcareous sand [6,7] for both the north and south site. Gulf Stream activity scours the bottom, limiting the water depth at which this sediment layer is observed. In Fig. 5, a seismic trace shows that the underlying limestone is exposed for water depths greater than 185 m for a particular track in the northern area. A seismic trace obtained during the LWAD FTE 96-2 experiment in the LWAD SCV 97 southern site [1] showed that the limestone was exposed at water depths greater than 160 m for the southern area. Based on the seismic data, site NS is the only one with significant sand cover. The thickness of the sand at the NS site was found to be at least 20 m based on light bulb drops [8].

Figures 6 through 9 show the BSS values from the various sites at 3.5, 3, 2.5, and 2 kHz as a function of grazing angle. Each curve or data point represents an average value over a set of 8 to 21 pings. The rock data (represented by symbols rather than curves) is a combination of data from

- different receiver beams,
- multiple deployments with different source and receiver depths, and
- repeated transmission sequences.

These realizations are plotted separately in the next section. The different beams and deployment depths produce different regimes of grazing angle, with the higher numbered beams (closer to broadside) producing lower grazing angles. To show the overall variability within the southern rock sites (SR1, SR2, and SR3), the data are presented as a scatter plot. For the north site observations, solid and dashed lines are used for the rock and sand data, respectively. For this experimental geometry, the grazing angles for the source-to-scatterer and scatterer-to-receiver are similar (i.e., within tenths of a degree), so only one angle needs to be considered in the analysis. The average of the two grazing angles is the quantity plotted on the x-axis of the scattering strength vs grazing angle figures.

In Figs. 6 to 9, the rock data show substantial variability within sites when all data sets are considered. Specifically, some SR1 and SR3 site data remain at a lower BSS level above 20 degrees grazing angle. Presumably a significant amount of variability arises from the fact that the ship drifted more than 1 knot during runs, so that within a run a track of several nautical miles was

sampled. The SR1 data that exhibited relatively low scattering were collected towards the end of the run when the ship had drifted into shallower water and may have encountered some sandy sediment cover. (The estimate of sand wedge extent shown in Fig. 3 is based on a few seismic tracks so it is not necessarily valid for the entire area.) Site SR3 data are generally several dB lower than data from sites SR1 and SR2 - the reasons are unknown but may be related to reduced interface roughness or the possibility that the SR3 site lies in an area where sand cover is present at deeper water depths. (This site was not sampled by the seismic system or by light bulbs.)

Northern rock data (NR) tend to show levels similar to those of the highest-level southern rock data. All rock data (SR1, SR2, SR3, and NR) contrast strongly with the data from the sandy site (NS). This clearly shows the effect of the sediment cover in creating reduced scattering strength. At lower frequencies, the rock/sand contrast is somewhat reduced.

At two southern rock sites (SR1 and SR2), data were collected at 1500 Hz, as shown in Fig. 10. Only slight differences were seen for the two sites. As indicated in the section below on frequency dependence, the level seems to be unusually low in comparison with the 2000 Hz data. At the northern site, a limited amount of data were collected at 4000 Hz and the strong contrast between the sand and rock can be seen in Fig. 11.

Frequency Dependence and Model Fits

In the previous section, the site dependence at each measured frequency was shown to be consistent, showing the contrast between the relatively low levels of the clear sandy site (NS) and higher (SR2 and SR1 deeper water) and intermediate (SR3 and SR1 shallower water) levels of the rock sites. It is also interesting to observe the frequency dependence at each site. McCammon's survey article [2] finds that no frequency dependence has been established by historical data in this frequency band (1.5 to 4.0 kHz). For the LWAD SCV 97 data, a consistent increase in scattering strength with frequency was obtained for rock sites — a result that had also appeared to a limited extent in the LWAD FTE 96-2 data.

The scattering strength at various frequencies is plotted for the southern rock sites in Figs. 12 through 17, the northern rock site in Fig. 18, and the southern rock site in Fig. 19. The 1500 Hz data are noticeably separated from the other data. It is not well understood what the frequency dependence of scattering data should be, but it is unclear why this data should not be relatively similar to the 2000 Hz data. The 1500 Hz data are presented here with this caveat.

The remaining frequencies show a rather consistent increase of scattering strength encompassing a change of 5 dB over the 2 to 4 kHz band. In the plots of frequency dependence, a reference curve ("Mackenzie") showing Lambert's law with a coefficient of -27 dB is provided. This curve represents the standard input to Navy performance models, with the selection of the -27 dB value originating in the work of Mackenzie [9]. This reference curve takes the following form on a dB scale:

$$BSS = -27 + 10\log(\sin^2\theta). \tag{2}$$

In Refs. 1 and 2, bottom scattering data tend to be flatter and are better represented by assuming that the scattering is proportional to the sine of the grazing angle. On a dB scale, this is

$$BSS = \mu + 10\log(\sin\theta) \ , \tag{3}$$

where μ is the proportionality constant (converted to dB). In Figs. 12 to 22, this function has been plotted with selected values of μ (e.g., -25, -20, -15, -10). For the SR2 data (Fig. 12), it can be seen that the 2000 Hz data are close to a μ value of -20, while the 3500 Hz data are closer to -15. The results were similar 15 min later when multifrequency transmissions (i.e., transmitting all frequencies at the same time and processing separately) were used, as shown in Fig. 13. Figure 14 shows a lower grazing angle set that was obtained 2 hours after the Fig. 13 transmissions by lowering the source and receiver. This gave an opportunity to observe a decrease in scattering strength at lower grazing angles that follows the dependence on the sine of the angle.

For the SR1 site, it has already been demonstrated that the scattering levels changed during the performance of the run due to the drifting of the ship to the vicinity of the sand wedge. Figure 15 shows the first data collected at site SR1. The runs using single-frequency transmissions and multifrequency transmissions (both 1 hour later) are shown in Figs. 16 and 17. The μ values have fallen by about 5 dB, giving intermediate values between the rock-scattering levels seen in the deeper water and the sand-scattering levels of site NS. The frequency dependence for site SR1 is similar to that observed for site SR2.

The remaining rocky sites, SR3 (Fig. 18) and NR (Fig. 19), also display some frequency dependence. As stated above, the SR3 levels are relatively low, falling below a μ value of -20. The frequency dependence is slight for the NR data but still observable.

Frequency dependence for the NS site (Fig. 20) was unclear. Attenuation values of at least 1 dB/m are expected in the calcareous sand wedge at 2 kHz and above [10,11]. As a result, there is presumably no interaction with the underlying limestone at site NS, since the sediment thickness is at least 20 m. Therefore, the scattering results at site NS represent scattering within the sediment volume or with the water/sediment interface. For one set of FTE 96-2 site B data, a *decrease* in scattering strength with increasing frequency was observed [1]. The presence of a scattering layer within the sediment volume, acoustically encountered by the lower frequency signals but not by the higher frequency signals (due to the difference in attenuation) could produce this type of frequency dependence. Another data set in the vicinity of site B showed no frequency dependence, indicating that the structure within the sand layer was spatially variable. The LWAD SCV 97 data are more consistent with the latter data set (i.e., they are not frequency dependent).

Table 1 presents nominal values of μ, assuming the $\sin\theta$ model of Eq. (3). For modeling purposes, it is best to refer to the individual plots (Figs. 12 through 20) to obtain details of the scattering behavior (e.g., deviations from the $\sin\theta$ model, values at other frequencies). Table 1 represents an overview of the data set that allows for comparison of the nominal levels for the various sites. The values of Table 1 are comparable to historical data. McCammon [2] gives an average μ value of -18.7 ± 8.6 dB assuming $\sin\theta$ dependence for a group of data sets from rock, coarse sand, and shell bottoms. All the data associated with rock are within this interval. McCammon also gives -27.5 ± 6.8 dB as an average μ value assuming $\sin\theta$ for fine sand and silt bottoms. This is also comparable to the NS data from LWAD SCV 97.

Table 1 — Nominal Values of μ for LWAD SCV 97 Data Assuming Sin θ Model

Site	Bottom Type	Grazing Angles (deg)	Frequency (Hz)	Coefficient (μ)
SR1 (deeper)	Rock	10-22	2000	-14
			3500	-17
SR1 (shallower)	Rock (w/ Sand?)	10-30	2000	-21
			3500	-18
SR2	Rock	9-24	2000	-20
			3500	-15
SR3	Rock (w/ Sand?)	10-30	2000	-22
			3500	-20
NR	Rock	14-28	2000	-18
			3500	-16
NS	Sand	7-20	all	-25 to -30

Table 2 — Values of μ for LWAD SCV-97/LWAD FTE 96-2 Composite Assuming Sin θ Model

Site	Bottom Type	Grazing Angles (deg)	Frequency (Hz)	Coefficient (μ)
SR2 + site Q	Rock	8-50	3000	-17
		10-50	3500	-15

Comparison with LWAD FTE 96-2 Data

The modifications to the system for the LWAD SCV 97 test and the sound speed profile characteristics produced lower grazing angle results than did the previous LWAD FTE 96-2 test. The environmental conditions, in most cases, made it more difficult to get higher grazing angles than the previous test. Due to the similarity of bottom type, the experimental results are complementary, and consideration of the two experiments together allows for consideration of the scattering strength dependence over a wide range of grazing angles.

In Figs. 21 and 22, data from LWAD SCV 97 site SR2 are plotted alongside data from FTE 96-2 site Q for 3500 Hz and 3000 Hz respectively. The locations of these runs can be found in Fig. 3. The data from the two experiments both indicate a μ value of approximately -15 dB, although the SR2 and Q sites were 7 miles apart. At 3000 Hz, the LWAD SCV 97 data are about 2 dB lower in level, while the LWAD FTE 96-2 data remain at the same level. At 2000 Hz, the scattering levels for the SCV have dropped to $\mu = -20$ dB, while the LWAD FTE 96-2 levels are at about -16 dB. As stated above, the frequency dependence of the rock scattering is not well understood and model development efforts are underway.

Table 2 shows the μ values for the LWAD SCV 97/LWAD FTE 96-2 composite made from combining data from site SR2 and site Q. They are shown only for 3000 and 3500 Hz, since the discrepancy in level between the two experiments increased at lower frequencies. As seen in the table, the composites span a wide range of grazing angles.

Sand data are also available from both experiments, but the LWAD FTE 96-2 sand data are within the SCV southern site, while the SCV sand data are from the SCV northern site. Consequently, the sand sites from the different tests are more than 12 nmi apart. Figure 23 shows an example. The scattering levels tended to indicate μ values in the -25 to -30 dB range for both experiments.

SUMMARY

During LWAD SCV 97, bottom backscattering strengths were measured at five sites off the Carolina coast. The water depths at these sites ranged from 121 to 232 m. For sites with presumably minimal sand cover (i.e., the sites deeper than the sediment wedge), the scattering strengths were demonstrably higher than those of the site with significant (> 20 m) sand cover. At the latter site, the acoustic energy was significantly attenuated in the layer so that the strong scattering from the underlying limestone did not occur. In some runs starting in deeper water, the scattering strengths started to decrease and change grazing angle dependence as the scattering wedge area was approached. Data generally followed a $\sin\theta$ dependence on grazing angle and tended to increase from 2 to 5 dB over the 2000 to 3500 Hz band.

The LWAD SCV 97 measurements provided an opportunity to extend the bottom backscattering measurements performed during LWAD FTE 96-2 to lower grazing angles, and relative consistency was obtained when the closest sites from the two experiments were considered together. For unknown reasons, the frequency dependence in the LWAD SCV 97 was more apparent — this will need to be addressed by the rock-scattering geophysical models under development. The bottom scattering data in some LWAD SCV 97 sites indicated a possible transition from rock scattering strengths to sand-scattering strengths as the ship drifted near the expected location of the sand wedge. Based on the measurements obtained in the two experiments, we were able to present empirical models covering a wide range of grazing angles for rock areas and also present levels for sandy areas and rock/sand transition areas. The Long Bay site provides strong contrast between areas where the Navy standard (Mackenzie) is a good predictor of scattering level and other areas where it underpredicts bottom backscatter by a factor of 10 to 15 dB.

ACKNOWLEDGMENTS

This work was sponsored by the Office of Naval Research Littoral Warfare Advanced Development Project, LCDR Scott Tilden, Program Manager. We thank Jerome Richardson, Lillian Fields, and Elisabeth Kim of Planning Systems Incorporated for assistance with the data processing.

REFERENCES

1. R. J. Soukup and P. M. Ogden, "Bottom Backscattering Measured Off the South Carolina Coast During Littoral Warfare Advanced Development Focused Technology Experiment 96-2," NRL Memorandum Report 7140—97-7905, Naval Research Laboratory, Washington DC, April 28, 1997.
2. D. F. McCammon, "Low Grazing Angle Bottom Scattering Strength: Survey of Unclassified Measurements and Models and Recommendations for LFA Use (U)," *Journal of Underwater Acoustics(USN)* **43**(1)(Secret), 33-47, January 1993 (Unclassified). (Issue is Secret, article is Unclassified.)

3. R. J. Soukup and D. W. Edsall, "Bottom Backscattering Measured Southwest of Key West During Littoral Warfare Advanced Development Focused Technology Experiment 97-2," NRL Memorandum Report 7140—97-7977, Naval Research Laboratory, Washington, DC, September 30, 1997.

4. P. D. Mourad and D. R. Jackson, "A Model/Data Comparison for Low-frequency Bottom Backscatter," *J. Acoust. Soc. Am.* **94**(1), 344-358 (1993).

5. P. M. Ogden and F. T. Erskine, "Surface Scattering Measurements Using Broadband Explosive Charges in the Critical Sea Test Experiments," *J. Acoust. Soc. Am.*, **95**, 746-761 (1994).

6. C. K. Paull and W. P. Dillon, "Structure, Stratigraphy, and Geologic History of Florida-Hatteras Shelf and Inner Blake Plateau," *AAPG Bull.*, **64**, 339-358 (1980).

7. G. A. Kerr, P. J. Bucca, J. K. Fulford and S. W. Snyder, "Environmental Variability During the Littoral Warfare Advanced Development Sponsored Focused Technology Experiment (FTE 96-2)," NRL Memorandum Report 7140—97-8056, Naval Research Laboratory, Washington DC, August 8, 1997.

8. B. R. Gomes, J. K. Fulford and G. A. Kerr, "Environmental Variability During the Littoral Warfare Advanced Development Sponsored System Concept Validation Test (SCV 96-2)," NRL Memorandum Report (in preparation).

9. K. V. Mackenzie, "Bottom Reverberation for 530 and 1030 cps Sound in Deep Water," *J. Acoust. Soc. Am*, **33**, 1498-1504 (1961).

10. C. S. Clay and H. Medwin, *Acoustical Oceanography: Principles and Applications* (John Wiley and Sons, New York, 1977).

11. Stephen Snyder, North Carolina State University, private communication.

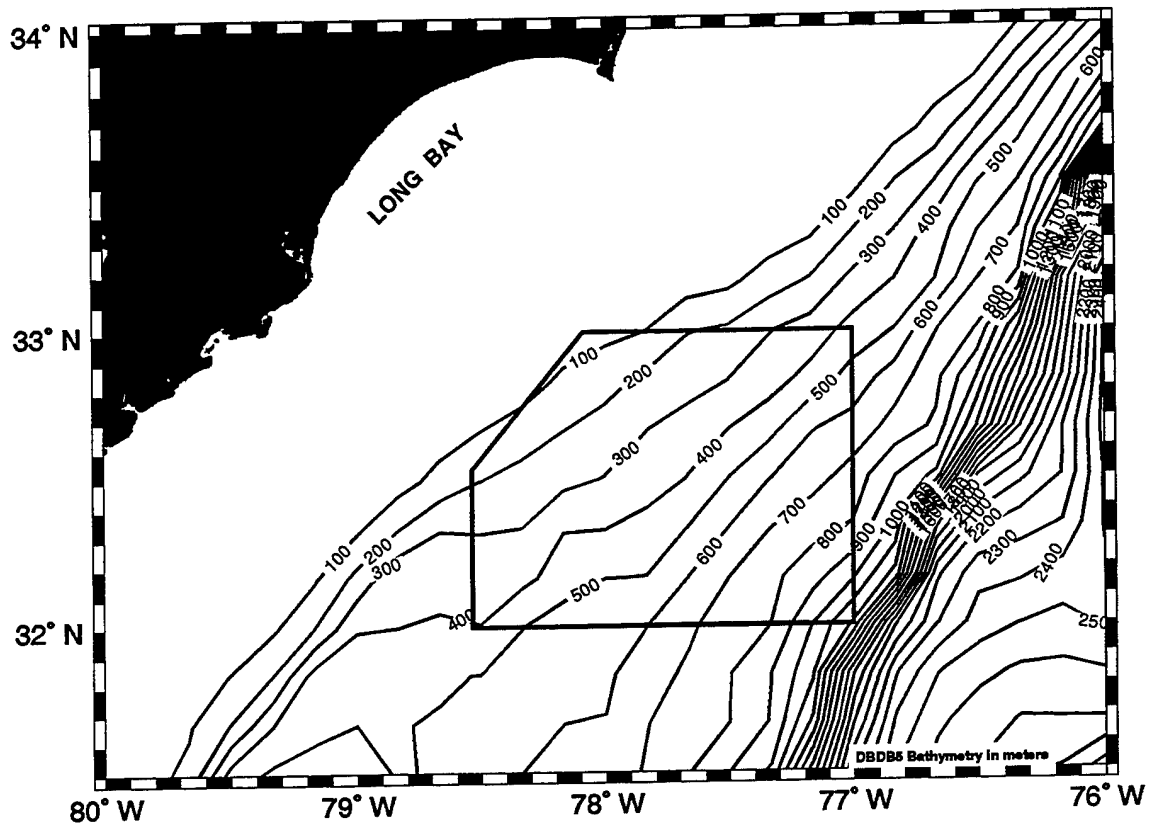

Fig. 1 — Bathymetric contours (in meters) in the vicinity of Long Bay, off the South Carolina coast. The box shows the LWAD SCV 97 test location, with most of the operations occurring at depths shallower than 300 m.

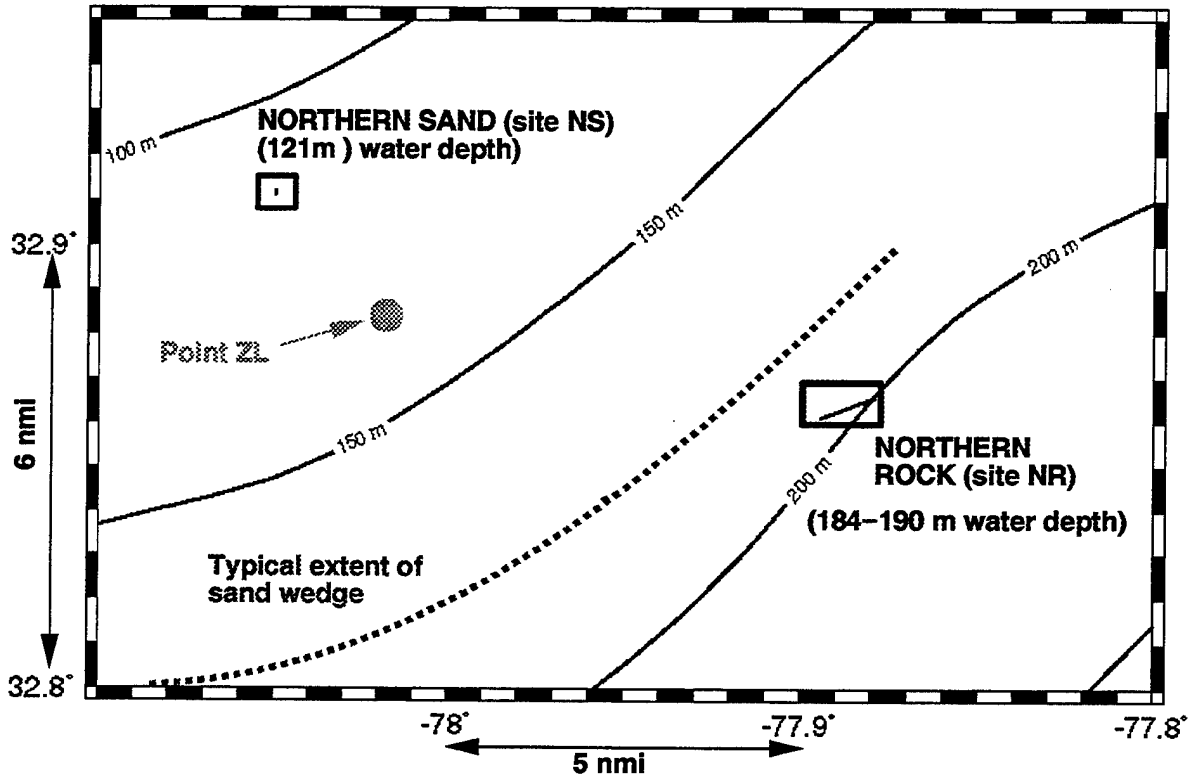

Fig. 2 — SCV-97 northern area bottom scattering experimental sites. The bathymetric contours are in meters (from the DBDB5 database), while the cited water depths for the sites were obtained from the ship's fathometer. The lines within the boxes represent the ship track during the scattering runs. A reference point for the deployment of other systems during the experiment (point ZL) is also shown.

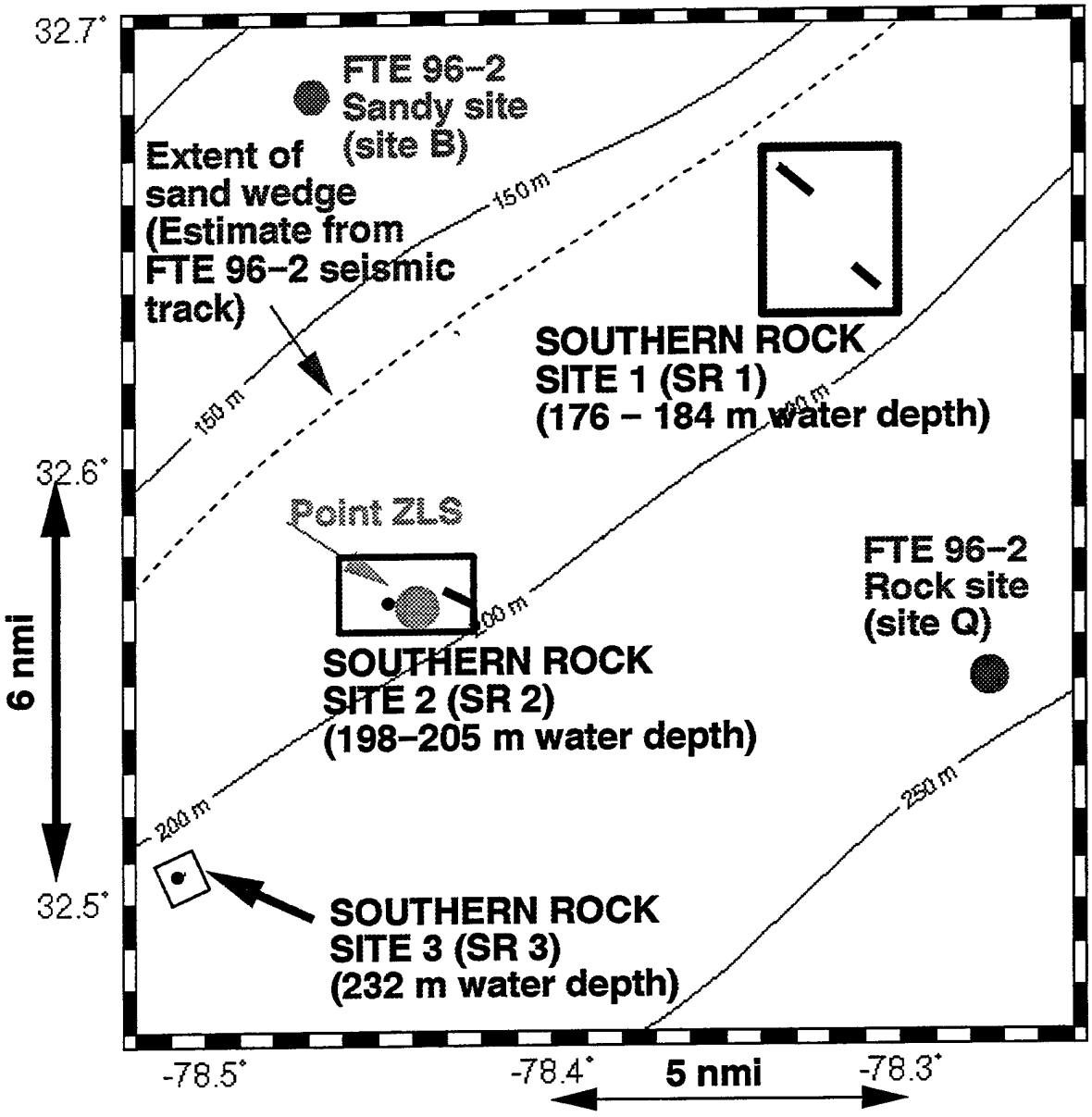

Fig. 3 — SCV-97 southern area bottom scattering experimental sites. The bathymetric contours are in meters (from the DBDB5 database), while the cited water depths for the sites were obtained from the ship's fathometer. The lines within the boxes represent the ship track during the scattering runs. A reference point for the deployment of other systems during the experiment (point ZL) is also shown.

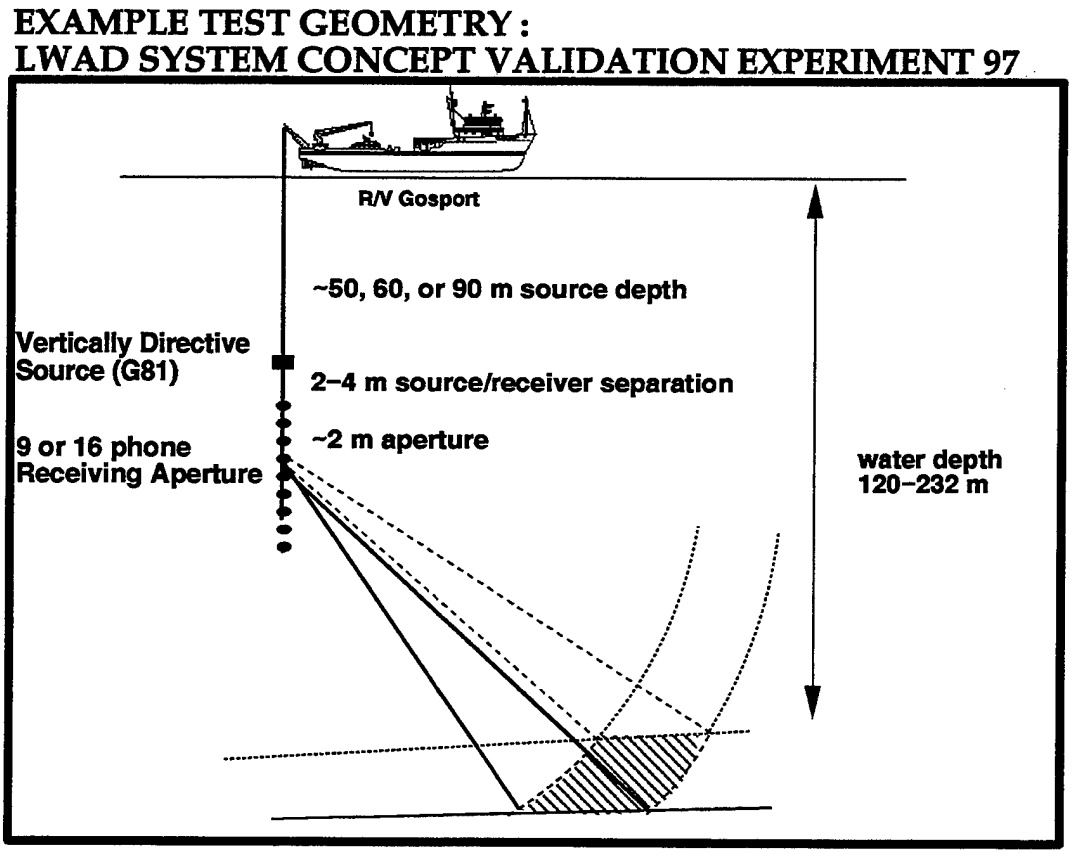

Fig. 4 — Depiction of the experimental geometry for bottom backscattering measurements in LWAD SCV 97. A sector of one receiver beam is shown and a sector of the scattering annulus is shaded.

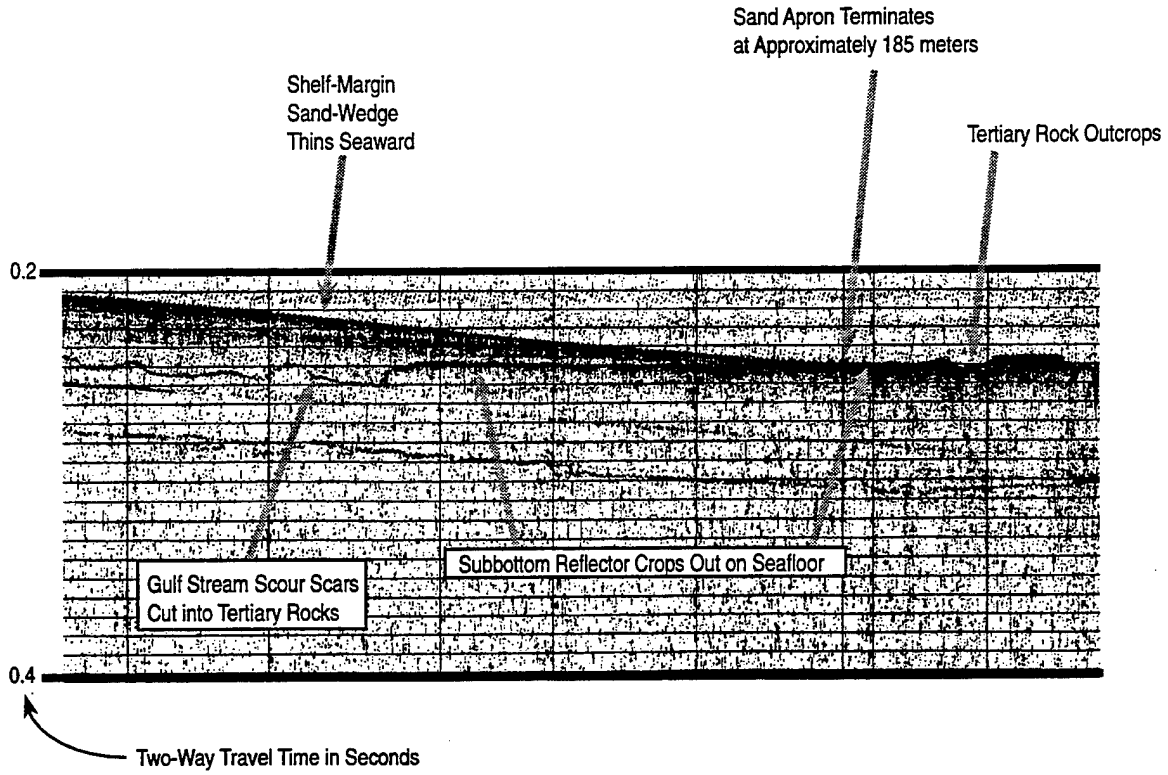

Fig. 5 — Seismic trace in the SCV northern site showing the termination of the sand cover. The track is about 135 deg true heading, so the water depth increases as the trace goes from left to right. (Figure provided by Dr. Stephen Snyder, North Carolina State University.)

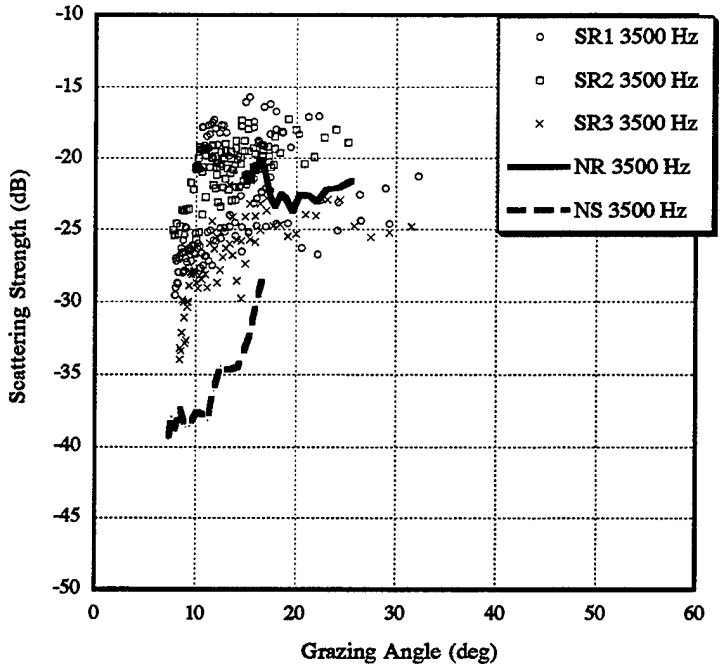

Fig. 6 — Bottom backscattering strength as a function of grazing angle at 3500 Hz for LWAD SCV 97 scattering sites

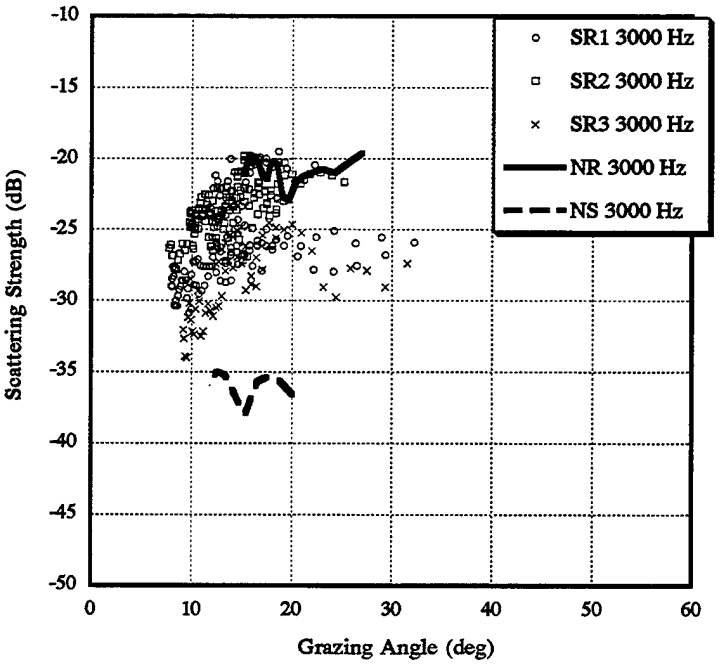

Fig. 7 — Bottom backscattering strength as a function of grazing angle at 3000 Hz for LWAD SCV 97 scattering sites

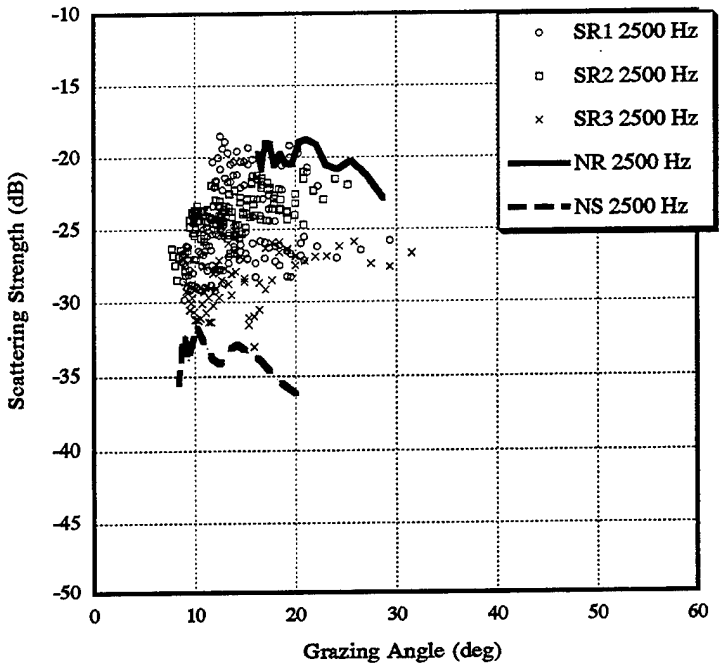

Fig. 8 — Bottom backscattering strength as a function of grazing angle at 2500 Hz for LWAD SCV 97 scattering sites

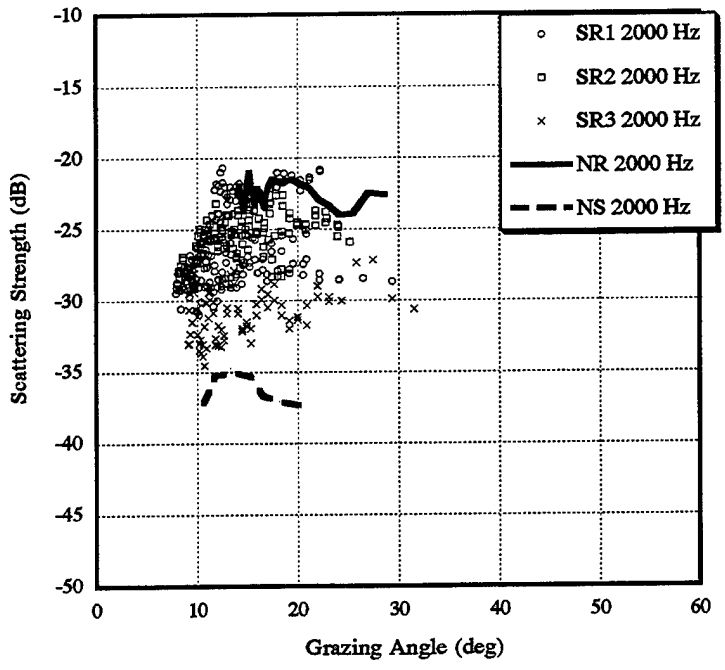

Fig. 9 — Bottom backscattering strength as a function of grazing angle at 2000 Hz for LWAD SCV 97 scattering sites

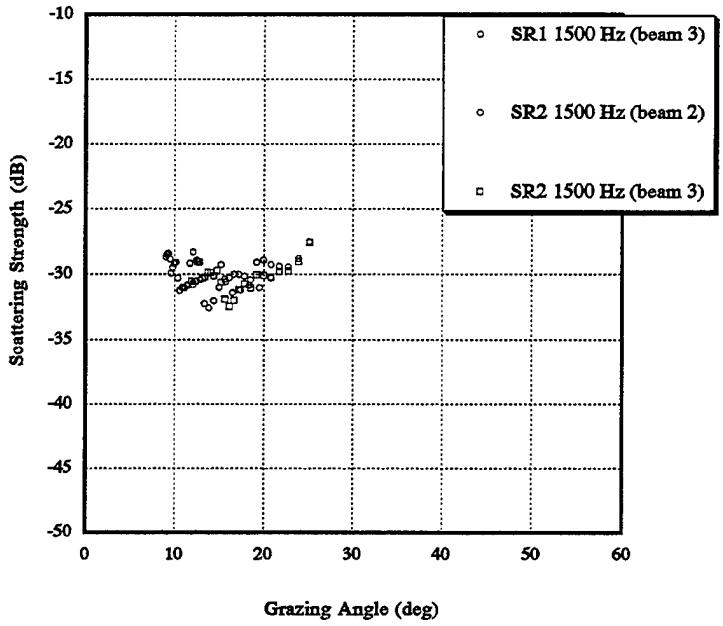

Fig. 10 — Bottom backscattering strength as a function of grazing angle at 1500 Hz for LWAD SCV 97 scattering sites

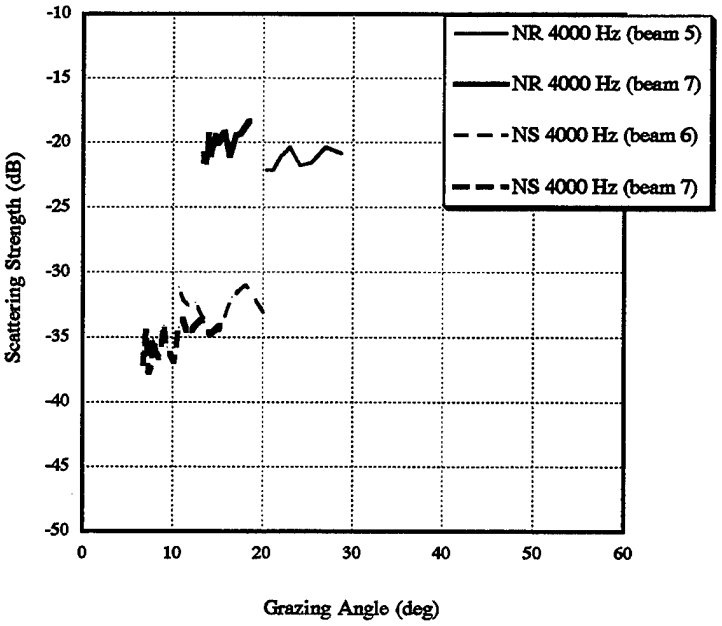

Fig. 11 — Bottom backscattering strength as a function of grazing angle at 4000 Hz for LWAD SCV 97 scattering sites

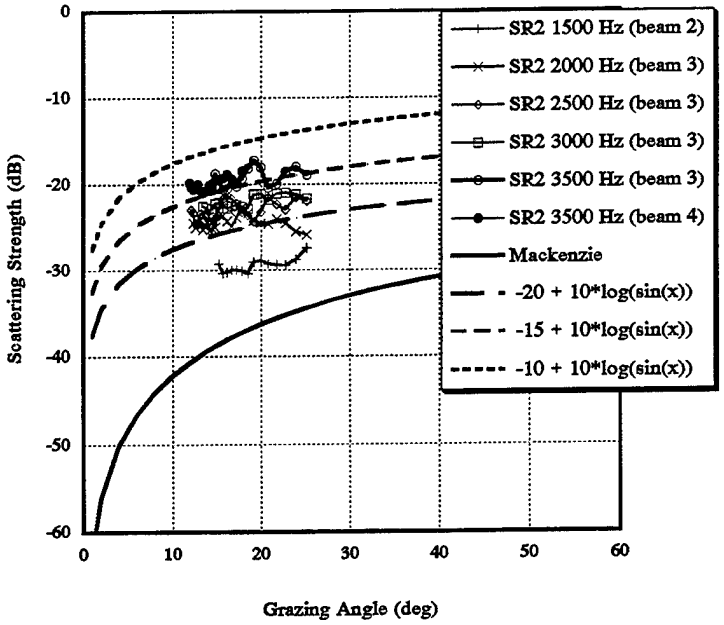

Fig. 12 — Bottom backscattering strength as a function of grazing angle for site SR2 at various frequencies with the source deployed at 50 m depth. The Mackenzie curve and other functions are also shown for comparison. Note the change in scale from the previous scattering strength plots.

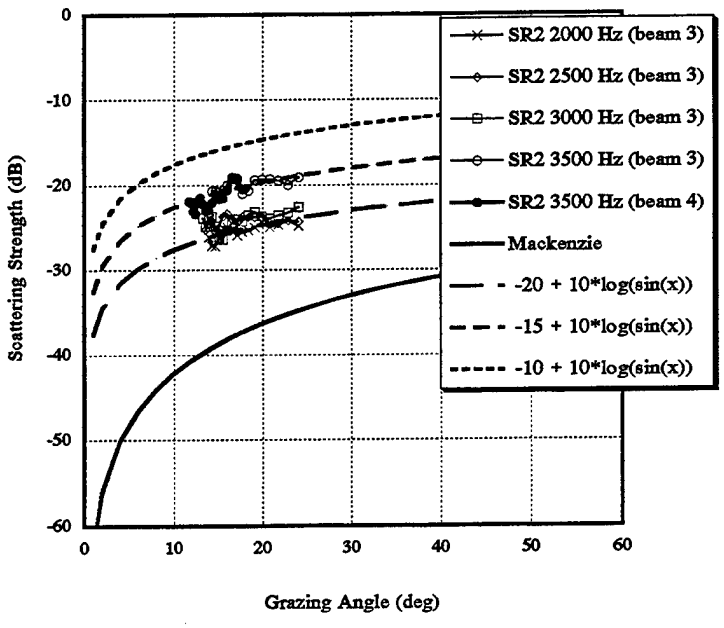

Fig. 13 — Bottom backscattering strength as a function of grazing angle for site SR2 at various frequencies with the source deployed at 50 m depth. These data were obtained 15 min later than the data in the previous plot. The Mackenzie curve and other functions are also shown for comparison.

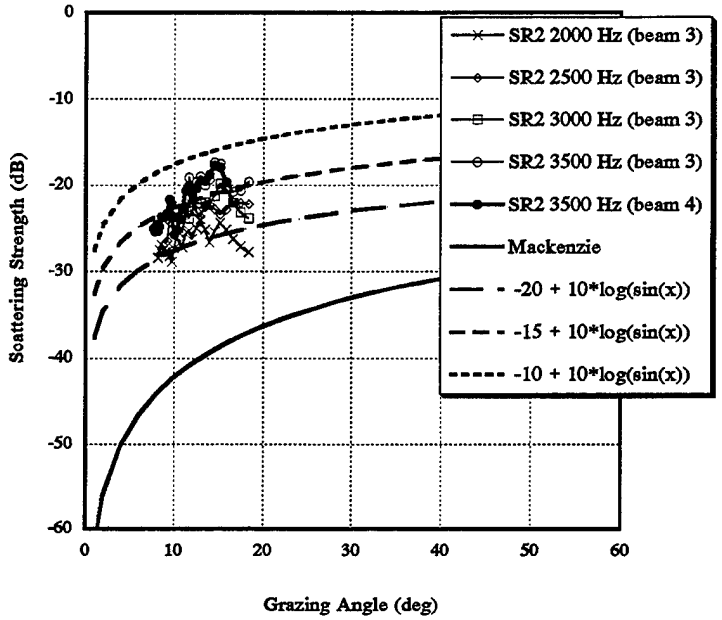

Fig. 14 — Bottom backscattering strength as a function of grazing angle for site SR2 at various frequencies with the source deployed at 90 m depth. These data were obtained 2 hours later than the data in the previous plot. The Mackenzie curve and other functions are also shown for comparison.

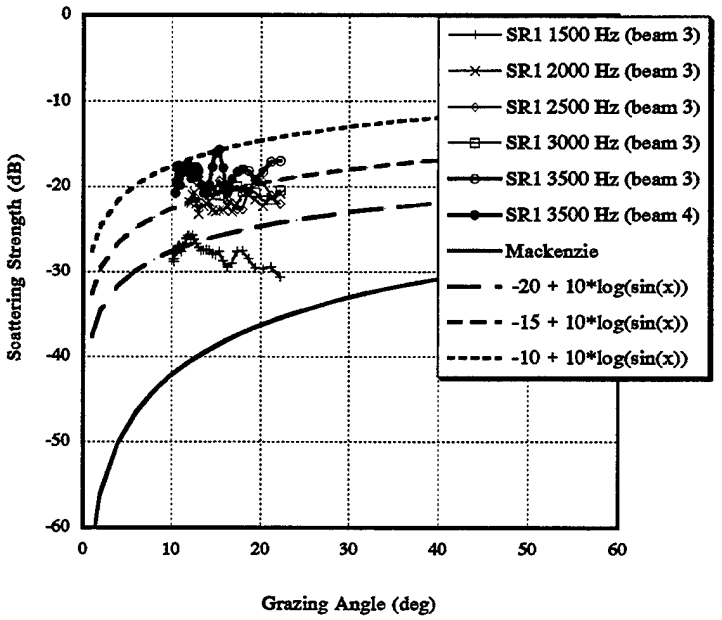

Fig. 15 — Bottom backscattering strength as a function of grazing angle for site SR1 at various frequencies with the source deployed at 50 m depth. The Mackenzie curve and other functions are also shown for comparison.

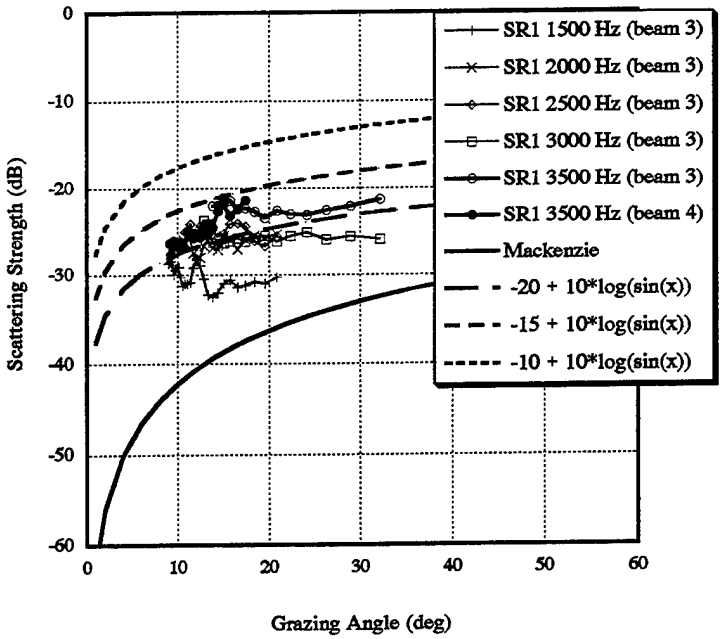

Fig. 16 — Bottom backscattering strength as a function of grazing angle for site SR1 at various frequencies with the source deployed at 90 m depth. These data were obtained 1 hour later than the data in the previous plot. The Mackenzie curve and other functions are also shown for comparison.

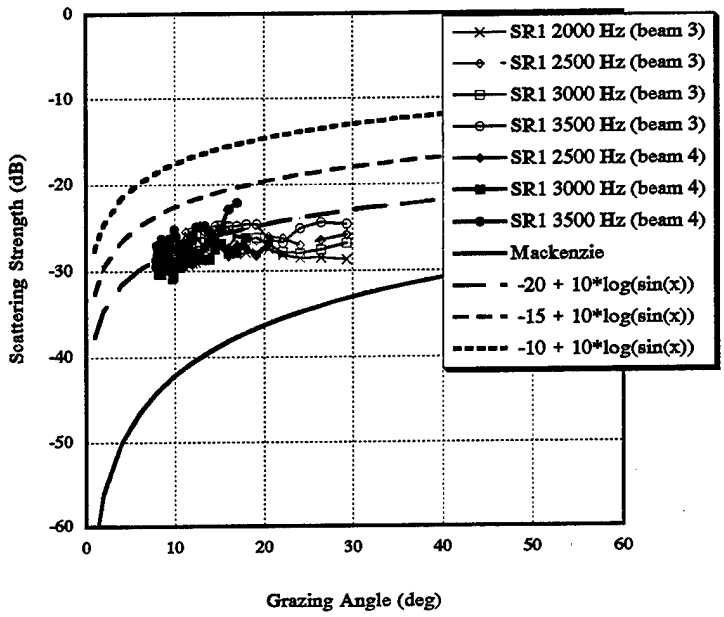

Fig. 17 — Bottom backscattering strength as a function of grazing angle for site SR1 at various frequencies with the source deployed at 90 m depth. These data were obtained 15 min later than the data in the previous plot. The Mackenzie curve and other functions are also shown for comparison.

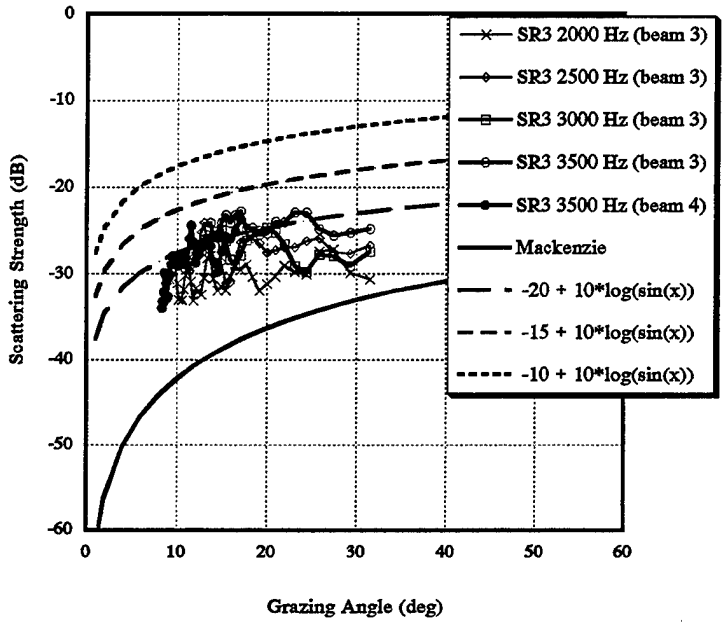

Fig. 18 — Bottom backscattering strength as a function of grazing angle for site SR3 at various frequencies with the source deployed at 90 m depth. The Mackenzie curve and other functions are also shown for comparison.

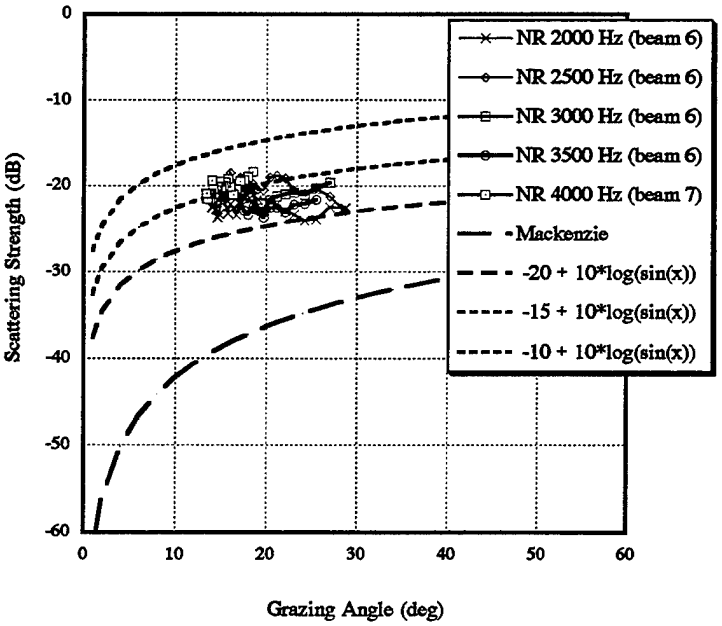

Fig. 19 — Bottom backscattering strength as a function of grazing angle for site NR at various frequencies with the source deployed at 60 m depth. The Mackenzie curve and other functions are also shown for comparison.

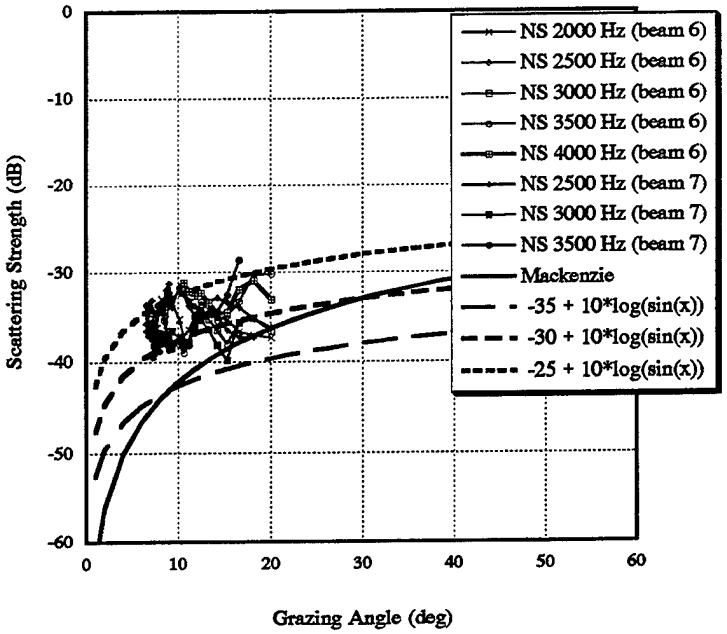

Fig. 20 — Bottom backscattering strength as a function of grazing angle for site NS at various frequencies with the source deployed at 90 m depth. The Mackenzie curve and other functions are also shown for comparison. Note that the constants of these functions (-35, -30, and -25) have been lowered relative to all previous scattering strength plots.

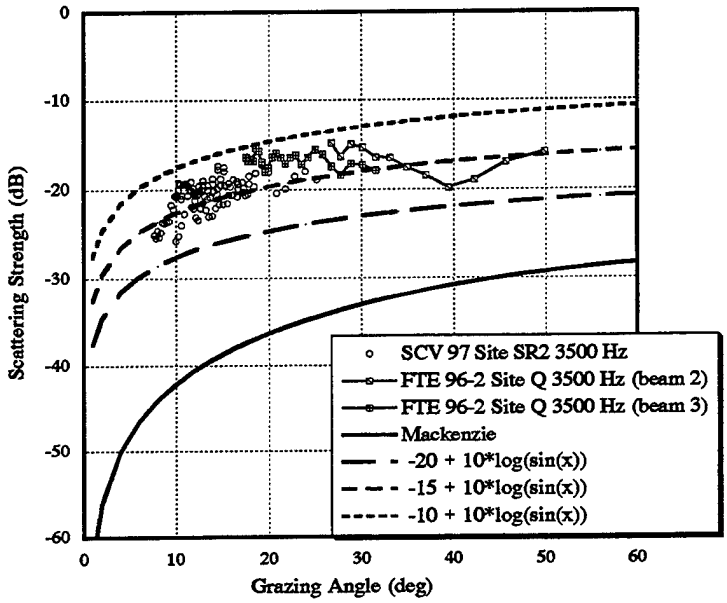

Fig. 21 — Bottom backscattering strength as a function of grazing angle compiled from LWAD SCV 97 data from site SR2 and FTE 96-2 data from site Q at 3500 Hz

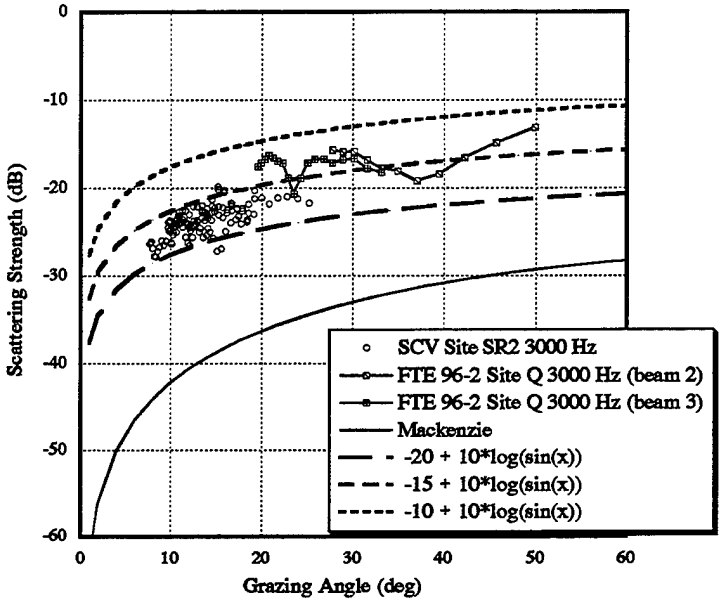

Fig. 22 — Bottom backscattering strength as a function of grazing angle compiled from LWAD SCV 97 data from site SR2 and FTE 96-2 data from site Q at 3000 Hz

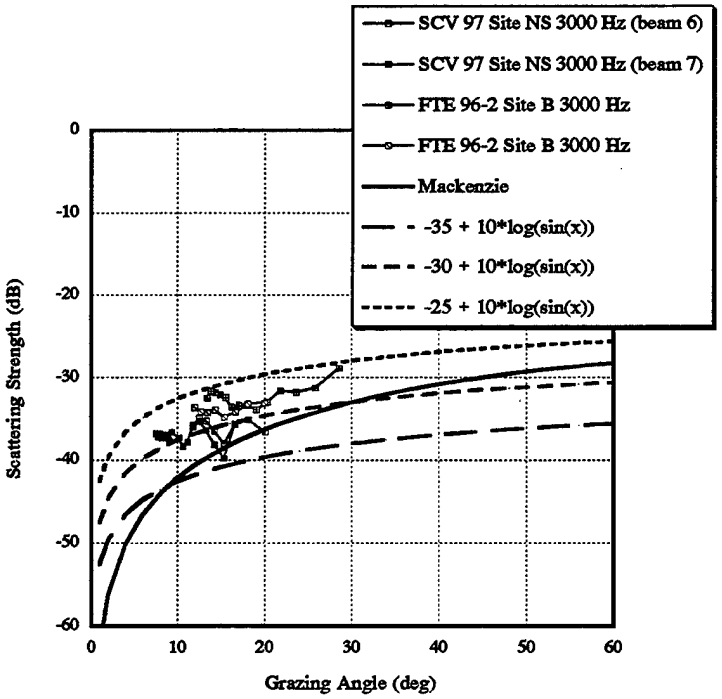

Fig. 23 — Bottom backscattering strength as a function of grazing angle compiled from LWAD SCV 97 data from site NS and FTE 96-2 data from site B at 3000 Hz